Supplemental online material

1D $Cs_2AgBr_3:Mn^{2+}$ crystals to Realize High Resolution X-ray Scintillation Imaging

Tao Chen,[a,#] Dedan Mu,[d,#] Feng Lin,[c,#] Wenjun Tang,[e] Yuqing Zhou,[a] Xinyue Shi,[a] Changjiang Li,[a] Xuekai Jiang,[a] Xin Li,[d] Haiyuan Chen,[e] Tao Chen,*[b], Xuhui Xu*[d] and Chong Wang*[c]

[a]Key Laboratory of Inorganic Functional Materials and Huangshan Technology Innovation Center for Green Chemical Engineering and New Materials, School of Chemistry and Chemical Engineering, Huangshan University, Huangshan, 245041, P. R. China

[b]Department of Materials Science and Engineering, School of Chemistry and Materials Science, University of Science and Technology of China, Hefei 230026, P. R. China
Email: tchenmse@ustc.edu.cn (T. Chen)

[c]Yunnan Key Laboratory of Electromagnetic Materials and Devices, School of Materials and Energy, Yunnan University, Kunming 650500, P. R. China
Email: cwang@ynu.edu.cn (C. Wang)

[d]School of Materials Science and Engineering, Kunming University of Science and Technology, Kunming 650093, P. R. China
Email: xuxuh07@kust.edu.cn (X. H. Xu)

[e]School of Materials and Energy, University of Electronic Science and Technology of China, Chengdu 611731 P. R. China

[#]These authors contributed equally to this work.

Experimental Section

Materials

Cesium bromide (CsBr) (99.9%), manganese (II) bromide hydrate ($MnBr_2 \cdot 4H_2O$) (98%) and silver bromide (AgBr) (＞99%) were purchased from Macklin. Hypophoaphoeous acid (H_3PO_2, 50 wt.% in H_2O) was purchased from Macklin. Acetone (C_3H_6O) was purchased from Keshi Chemical Technology (99.5%). Hydriodic acid (HBr 48 wt.%) aqueous solution was purchased from Macklin.

The synthesis of Cs_2AgBr_3 crystals and Mn^{2+}-doped Cs_2AgBr_3 crystals

Cs_2AgBr_3 crystals were synthesized by mixing 8 mmol CsBr (1.7025 g) and 4 mmol AgBr (0.75108 g) and 200 μL H_3PO_2 into 6.5 mL HBr acid solution. The whole solution was heated to 100 °C and stirred for 6-8 hours to make all the solutes totally dissolved. Subsequently, the solution was slowly cooled at a cooling speed of 6 °C/h to room temperature. Large quantities of Cs_2AgBr_3 crystals were precipitated from the solution. After reaction, Cs_2AgBr_3 crystals were washed with acetone for several times to remove all the surface impurities. Finally, Cs_2AgBr_3 crystals were dried at oven at 50 degrees for further characterization and tests. The synthetic procedures of Mn^{2+} doped Cs_2AgBr_3 crystals are identical to the Cs_2AgBr_3 synthetic process except for partially replacing the Ag^+ atoms with Mn^{2+} atoms with the molar ratios of 2.5%, 5%, 7.5%, 10%, respectively.

The Cs_2AgBr_3:5%Mn^{2+}@PMMA composite film fabrication

1.6 g PMMA was added into 10 mL toluene, and stirred fiercely at 60 °C to make the PMMA totally dissolved. The Cs_2AgBr_3:5%Mn^{2+} crystals were hand-ground into powder, and subsequently 0.9 g Cs_2AgBr_3:5%Mn^{2+} powder was added into the PMMA solution and stirred for another 3 hours to obtain homogeneous solution. About 7 mL of the above prepared Cs_2AgBr_3:5%Mn^{2+}@PMMA composite colloids were dropped and coated on a pre-cleaned flat glass-plate. And finally, the plate was put on the heating

plate at 50 °C for 8 hours to remove the organic solvents. After drying, peeling off the Cs_2AgBr_3:5%Mn^{2+}@PMMA composite film from the glass-plate carefully for tests.

DFT Calculations

All spin-polarized DFT calculations were performed using the Vienna Ab initio Simulation Package (VASP)[1] based on the generalized gradient approximation of the Perdew−Burke−Ernzerhof functional.[2] The interactions between core and valence electrons were described by the projector-augmented wave method[3] with a plane wave energy cutoff of 550 eV. The total energy tolerance was 10^{-7} eV, and the force tolerance was 0.01 eV $Å^{-1}$. The electronic occupancies were determined by Gaussian smearing with a smearing width of 0.10 eV. The spin-polarization incorporated within the calculations indeed facilitates the consideration of spin-biasing effects. Dipole corrections were added along the z-direction. The DFT-D3 method of Grimme was used to calculate van der Waals corrections.[4] The data obtained was processed using VASPkit[5] to generate the results, and visualized using VESTA.[6]

Characterization Methods

XRD patterns of the samples were recorded on DX-2700BH X-ray diffractometer with a Cu Kα source. The UV-vis absorption spectra of the $Cs_3Cu_2I_5$ films were conducted at UV-Lambda 650s UV-vis spectrometer. The steady-state photoluminescence (PL) spectra and time-resolved PL (TRPL) decay were recorded on FLS1000 (UK) with an excitation wavelength of 366 nm. The time-resolved PL decay curves were fitted by a double exponential equation:

$$I(t) = I_0 + A_1\exp\left(\frac{-t}{\tau_1}\right) + A_2 exp\left(\frac{-t}{\tau_2}\right)$$

where I is the luminescence intensity, t is the time, A_1 and A_2 are fitting constants, and the short and long fluorescence lifetimes of the exponential component are denoted as τ_1 and τ_2, respectively. The average lifetime is calculated by:

$$\tau_{ave} = \frac{A_1 * \tau_1^2 + A_2 * \tau_2^2}{A_1 * \tau_1 + A_2 * \tau_2}$$

The RL spectra were tested using Ocean insight QE pro fluorescence spectrometer.

Power dependence PL spectra were performed on Horiba LabSpec 6 with an optical power meter.

Table S1. The results of ICP-MS measurements

Molar feed ratio of $n_{(Mn^{2+})}/n_{(Ag^{+})}$	**Actual molar ratio $n_{(Mn^{2+})}/n_{(Ag+)}$**
1: 39	0.23%
1:19	0.48%
3:37	0.71%
1:9	0.95%

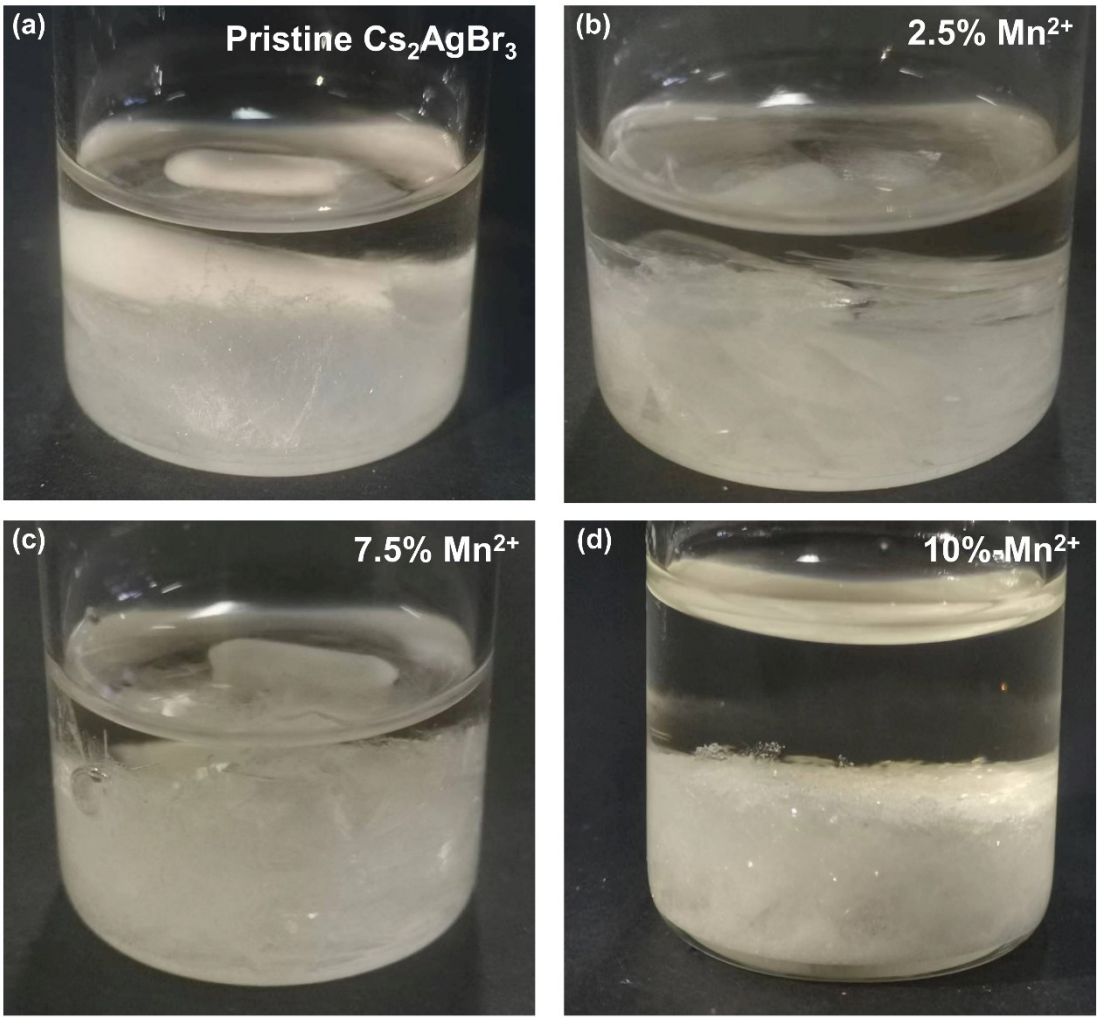

Figure S1. The Photographs of Cs_2AgBr_3 crystals with different Mn^{2+} ion doping concentrations in HBr aqueous solution. (a) pristine Cs_2AgBr_3 crystals; The Mn^{2+} ion

doping concentrations for other samles: (b) 2.5%; (c) 7.5%; (d) 10%.

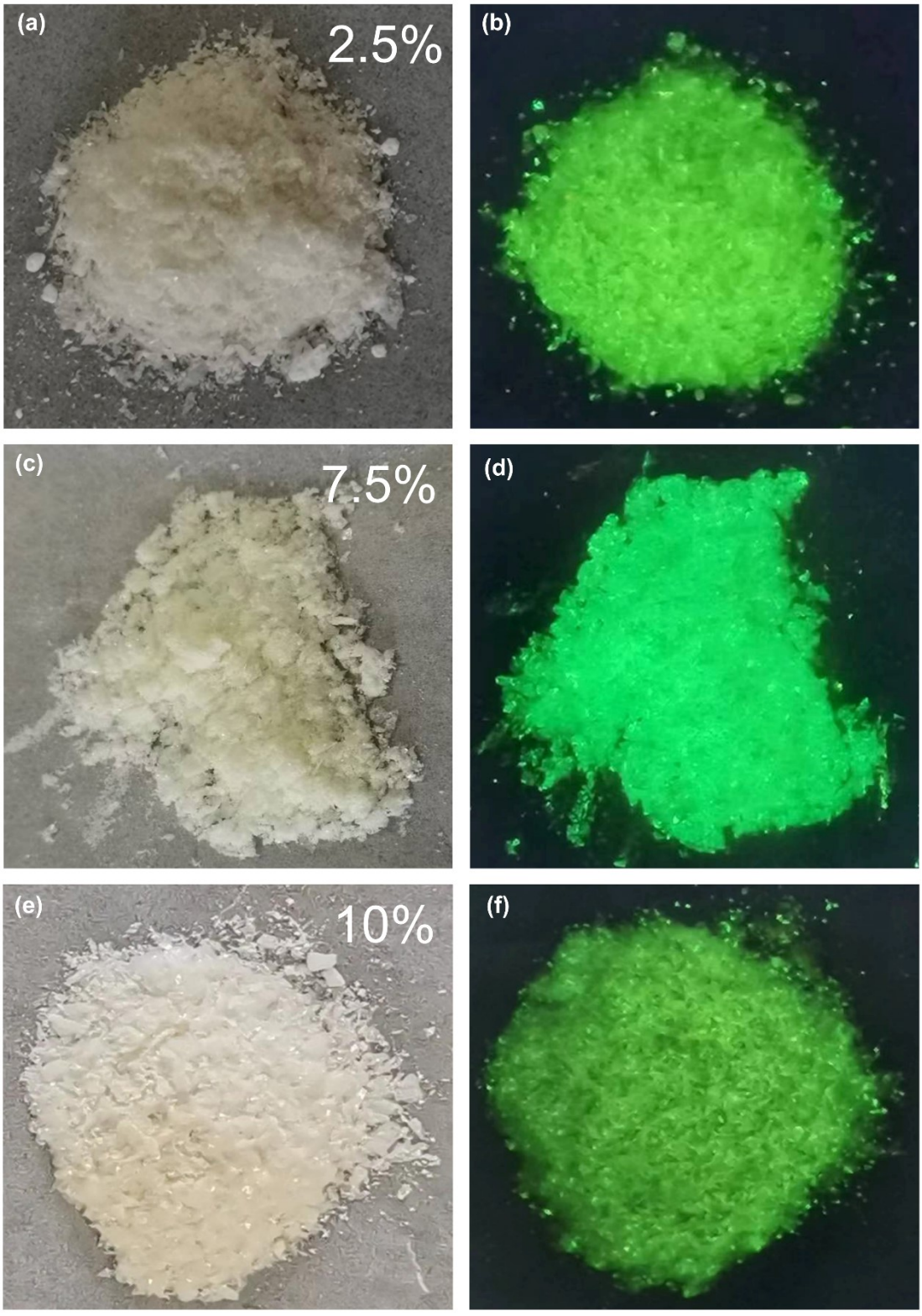

Figure S2. Photographs of Cs_2AgBr_3:xMn^{2+} crystals under visible light and UV light. The Mn^{2+}-doped Cs_2AgBr_3 samples with different doping contents: (a, b) 2.5%; (c, d) 7.5%; (e, f) 10%.

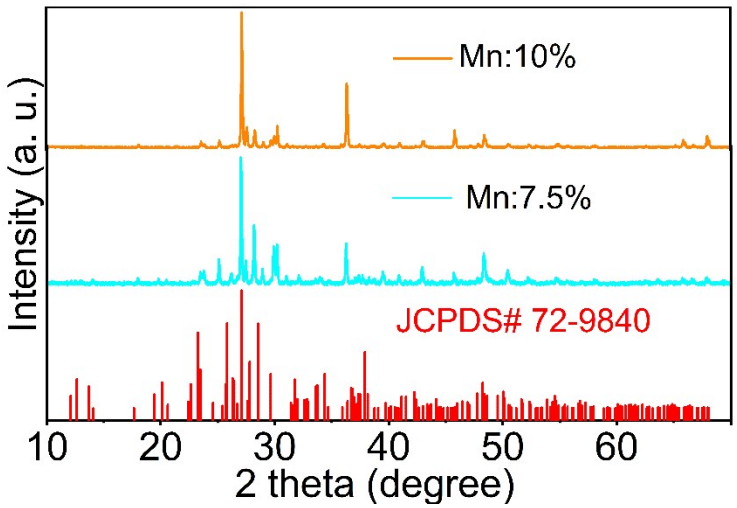

Figure S3. PXRD spectra of Cs_2AgBr_3:xMn^{2+} crystals.

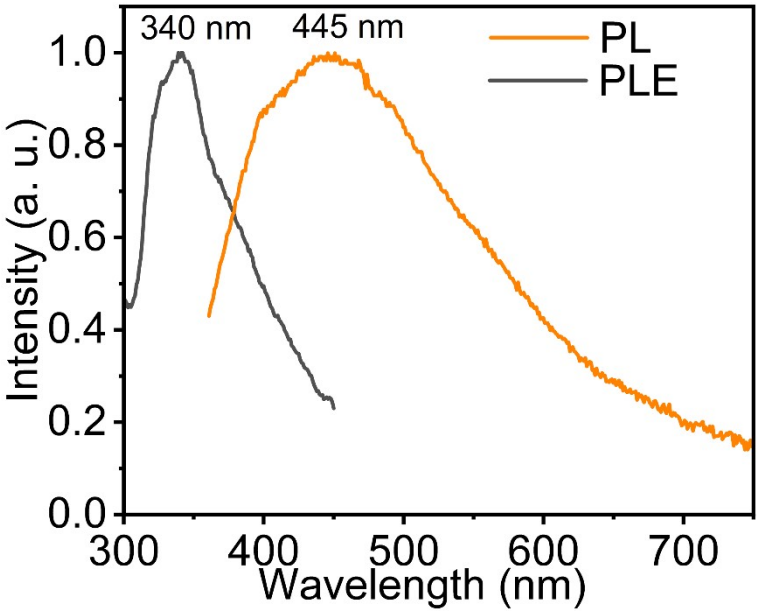

Figure S4. PL and PLE spectra of pristine Cs_2AgBr_3.

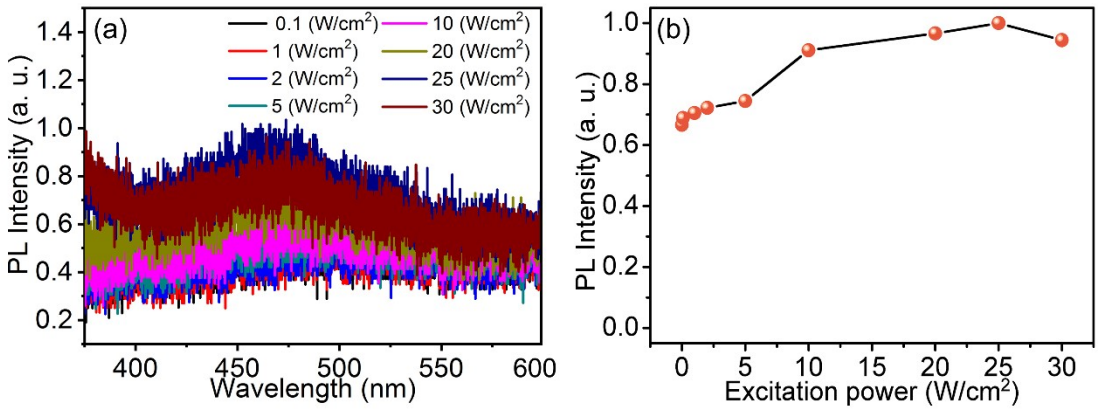

Figure S5. (a) Excitation power dependent PL spectra for pristine Cs_2AgBr_3. (b) The corresponding plots of the PL intensity versus excitation power, excitation source: 325 nm laser.

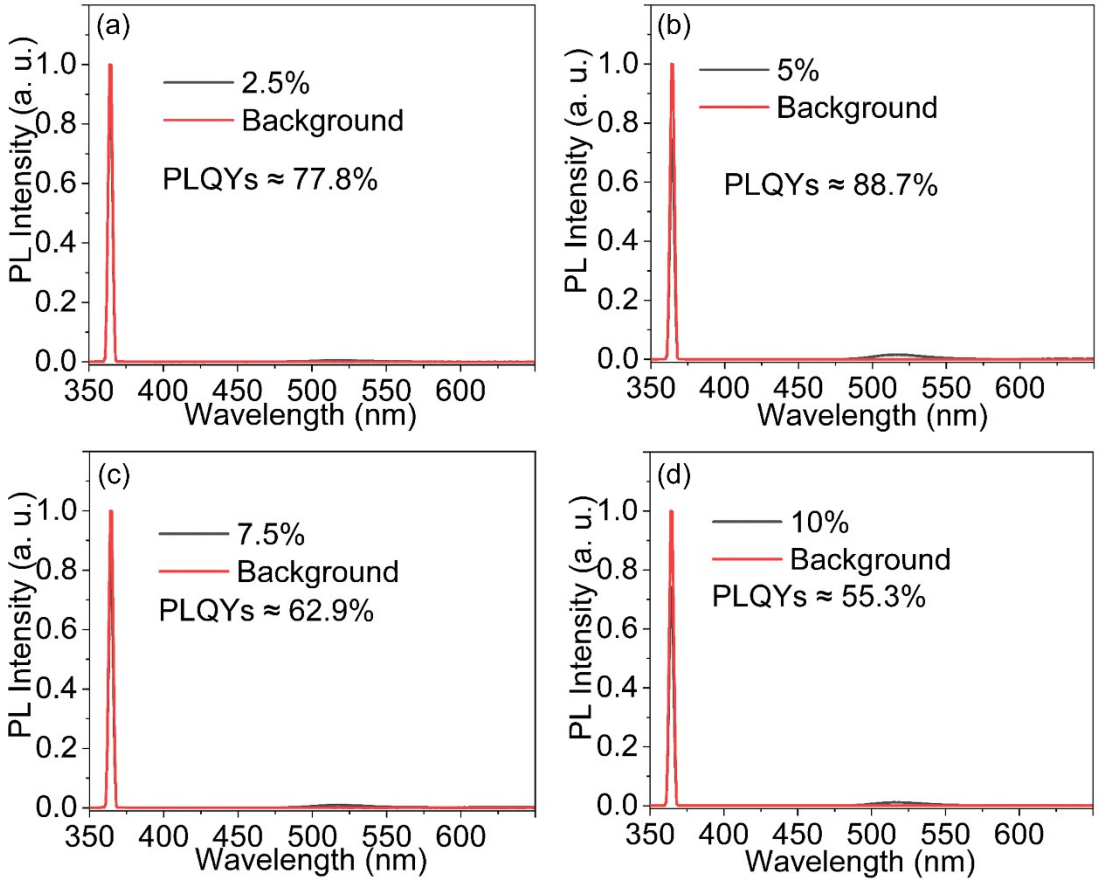

Figure S6. Absolute photoluminescence quantum yield measurements of (a) pristine Cs_2AgBr_3 crystals and Cs_2AgBr_3 crystals with different Mn^{2+} doping contents: (b) 2.5%; (c) 5%; (d) 7.5%; (e) 10%.

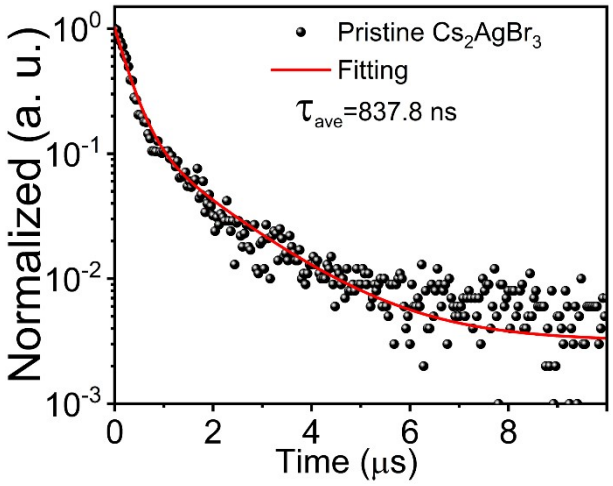

Figure S7. Time-resolved PL decay curve of pristine Cs_2AgBr_3.

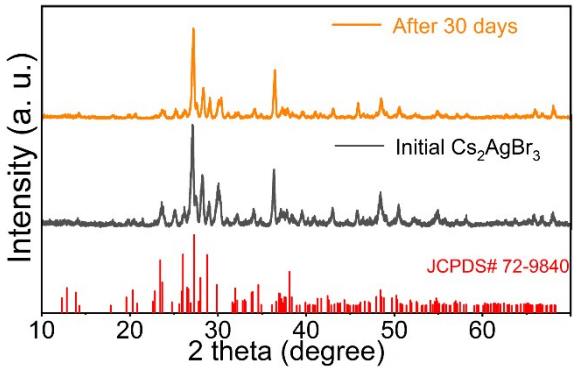

Figure S8. PXRD spectra of Cs_2AgBr_3:5%Mn^{2+} crystal when it was exposed in air for 30 days.

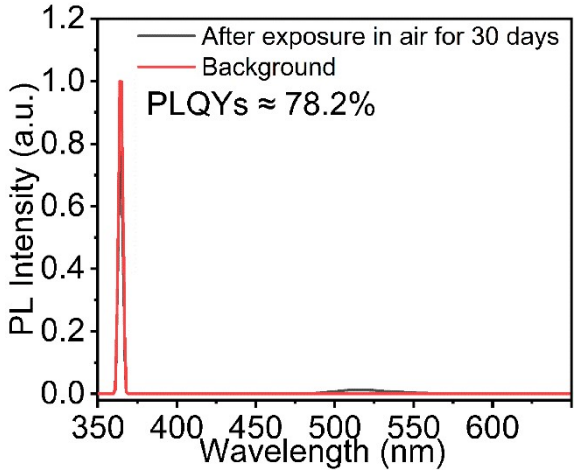

Figure S9. PLQYs of Cs_2AgBr_3:5%Mn^{2+} crystal when it was exposed in air for 30 days.

Table S2. Performance comparisons of metal halide perovskite–based scintillators.

Materials	Maximum emission (nm)	Detection limits (nGy_{air}/s)	Decay time (excited source)	Resolution (lp/mm)	Ref.
$Cs_2Ag_{0.6}Na_{0.4}In_{1-y}Bi_yCl_6$	605-652	19	2800 ns (400 ns)	4.3 MFT=0.2	[1][7]
Rb_2AgBr_3	480	19	5.31 ns (^{22}Na, 511 keV)	10.2 MFT=0.2	[2][8]
$(C_8H_{17}NH_3)_2SnBr_4$	596	/	3340 ns (350 nm)	200 μm (5 lp/mm)	[3][9]
$Cs_3Cu_2I_5$:Mn	450 and 565	49	/	11.8	[4][10]
$Cs_3Cu_2I_5$	445	48.6	969±9.6 ns	17 MFT=0.2	[5][11]
$Cs_3Cu_2I_5$	525	81.7	108500 ns	9.6 MFT=0.2	[6][12]
$(PPN)_2SbCl_5$	635	191.4	4100 ns (635 nm)	/	[7][13]
$Cs_4MnBi_2Cl_{12}$	610	/	49000 ns	/	[8][14]
$(C_{38}H_{34}P_2)MnBr_4$	517	72.8	318000 ns	322 μm	[9][15]
$CsCu_2I_3$	570	/	~1186 ns	/	[10][16]
$Cs_2CdBr_2Cl_2$	495	17.82	70740 ns	12.3	[12][17]
$(TPPen)_2Mn_{0.9}Zn_{0.1}Br_4$	515	204.1	298040 ns	11.2	[13][18]
Cs_2HfCl_6	427 and 447	55	4860 and 12290 ns	11.2	[14][19]
Cs_2AgBr_3:Mn	519	478.8	255.2 μs	24	This work

References

1. S. Grimme, J. Antony, S. Ehrlich and H. Krieg, *J. Chem. Phys.*, 2010, **132**, 154104.
2. G. Kresse and J. Furthmüller, *Phys. Rev. B*, 1996, **54**, 11169-11186.
3. H. Niu, Z. Zhang, X. Wang, X. Wan, C. Shao and Y. Guo, *Adv. Funct. Mater.*, 2020, **31**, 2008533.
4. J. P. Perdew, K. Burke and M. Ernzerhof, *Phys. Rev. Lett.*, 1996, **77**, 3865-3868.
5. V. Wang, N. Xu, J.-C. Liu, G. Tang and W.-T. Geng, *Comput. Phys. Commun.*, 2021, **267**, 108033.
6. K. Momma and F. Izumi, *J. Appl. Crystallogr.*, 2008, **41**, 653-658.
7. W. Zhu, W. Ma, Y. Su, Z. Chen, X. Chen, Y. Ma, L. Bai, W. Xiao, T. Liu, H. Zhu, X. Liu, H. Liu, X. Liu and Y. Yang, *Light: Sci. Appl.*, 2020, **9**, 112.
8. M. Zhang, X. Wang, B. Yang, J. Zhu, G. Niu, H. Wu, L. Yin, X. Du, M. Niu, Y. Ge, Q. Xie, Y. Yan and J. Tang, *Adv. Funct. Mater.*, 2021, **31**, 2007921.
9. J. Cao, Z. Guo, S. Zhu, Y. Fu, H. Zhang, Q. Wang and Z. Gu, *ACS Appl. Mater. Interfaces*, 2020, **12**, 19797-19804.
10. B. Wang, X. Ouyang, X. He, Z. Deng, Y. Zhou and P. Li, *Adv. Opt. Mater.*, 2023, **11**, 2300388.
11. J.-X. Wang, X. Wang, J. Yin, L. Gutiérrez-Arzaluz, T. He, C. Chen, Y. Han, Y. Zhang, O. M. Bakr, M. Eddaoudi and O. F. Mohammed, *ACS Energy Lett.*, 2021, **7**, 10-16.
12. Q. Zhou, J. Ren, J. Xiao, L. Lei, F. Liao, H. Di, C. Wang, L. Yang, Q. Chen, X. Yang, Y. Zhao and X. Han, *Nanoscale*, 2021, **13**, 19894-19902.
13. Q. He, C. Zhou, L. Xu, S. Lee, X. Lin, J. Neu, M. Worku, M. Chaaban and B. Ma, *ACS Mater. Lett.*, 2020, **2**, 633-638.
14. J.-H. Wei, J.-F. Liao, X.-D. Wang, L. Zhou, Y. Jiang and D.-B. Kuang, *Matter*, 2020, **3**, 892-903.
15. L.-J. Xu, X. Lin, Q. He, M. Worku and B. Ma, *Nat. Commun.*, 2020, **11**, 4329.
16. S. Cheng, A. Beitlerova, R. Kucerkova, E. Mihokova, M. Nikl, Z. Zhou, G. Ren and Y. Wu, *ACS Appl. Mater. Interfaces*, 2021, **13**, 12198-12202.
17. H. Xu, W. Liang, Z. Zhang, C. Cao, W. Yang, H. Zeng, Z. Lin, D. Zhao and G. Zou, *Adv. Mater.*, 2023, **35**, 2300136.
18. J. Jin, K. Han, Y. Hu and Z. Xia, *Adv. Opt. Mater.*, 2023, **11**, 2300330.
19. F. Zhang, Y. Zhou, Z. Chen, X. Niu, H. Wang, M. Jia, J. Xiao, X. Chen, D. Wu, X. Li, Z. Shi and C. Shan, *Laser Photonics Rev.*, 2023, **17**, 2200848.